Development of a Combined Bulging-Piercing Technique to Reduce Forming Load for a Long Semi-Hollow Stepped Part

Nara Nakeenopakun
King Mongkut's University of Technology North Bangkok
Sutee Olarnrithinun
King Mongkut's University of Technology North Bangkok
Yingyot Aue-u-lan (yingyot.a@tggs.kmutnb.ac.th)
King Mongkut's University of Technology North Bangkok https://orcid.org/0000-0002-2925-4974

Research Article

Keywords: Combined bulging-piercing technique, Long semi-hollow stepped shafts, Hot backward extrusion, Forming load reduction, Hot forging process, FEM simulation

Posted Date: January 5th, 2022

DOI: https://doi.org/10.21203/rs.3.rs-1209394/v1

Abstract

This paper aims to develop a new forming technique to manufacture a long semi-hollow stepped part. Traditionally, hot backward extrusion is used. This technique is not suitable, because it requires a very high forming load acting on the die and punch especially at the contact between punch and workpiece. As a result, the service life of the punch is very low. Therefore, a new technique to overcome this problem is needed. A combined bulging-piercing technique was proposed and developed in this research. The main concept of this technique is to bulge the part by upsetting the workpiece between the punch and the counter-punch to generate high frictional contact pressure which will help to restrain the material sliding down to the die cavity during the piercing step. In other words, this technique utilizes frictional force at the die-workpiece interface to reduce the forming load of the punch. Finite element modeling was employed to investigate and determine the suitable level of the bulging which can reduce the forming load without generating any significantly high force to the counter-punch. Only experiments with the minimum forming load were selected and implemented to validate this concept, because other conditions with high load will risk to damage the punch and the machine press of the product line. The results show that this technique can reduce the forming load by almost 40%, and also control a good concentricity of the part and reduce the wall thickness variation.

1. Introduction

The success of the forging processes requires high tonnage of the press machine and high strength/toughness of tools/dies to deform the materials to the required shape or dimension. These result in high production costs and limits in manufacturing some of the part configurations.

To reduce the production cost, the reduction in the forming load and the tooling costs is a big and major challenge for engineers and researchers nowadays. In other words, the lower forming load could enhance the service life of the forming tools and lower press machine capacity. Many techniques were developed and introduced to overcome these problems by focusing on the design of billets, toolings, and processes. Many techniques for the forming load reduction are reviewed and some of them are instanced [1]. Relief hole and axis is a method of the divided flow technique proposed to reduce the forming load in a cold forging process of gears proposed by Kondo et al [2].The material flow is split into 2 parts to fill the tooth tips located at the outer gear teeth and/or flow either radially inwards toward the center axis or axially within a central hole simultaneously [3]. In addition, the optimization of the preform shape and modification of the final forged shape is a technique that can reduce the forming load and also facilitate the die filling, improve material yield, and eliminate forging defects. A modern forging process, which is the combination of the advantages of sheet forming and cold forging, was introduced, namely Flow Control Forming (FCF) [4] or Sheet-bulk metal forming (SBMF) [5]. The upsetting, ironing, and extrusion process are integrated into the conventional sheet metal forming which is typically the sheet forming consisting of the blanking, drawing, and bending processes. Therefore, the sheet material is forced to change shape at all 3-dimensions similar to the material flow in the bulk forming process. It is mentioned that this FCF or SBMF is mainly to reduce the material waste as well as the forming load [6]. Furthermore,

a technique for reducing the number of toolings for producing a similar product by only the few dimension differences, namely Common Single-Die Exchange Technique or C-SDET, is proposed [7]. The idea is to determine the representative preform that could be used to produce various product models. In other words, this design aims to develop common generalized preforms by using the same component configuration/shape but varying the dimensions in some places to decrease the number of preforms and tooling installation time (downtime of the machine to install the tooling for each model).

The design of the optimum preforms and tooling shapes requires specific knowledge and past experience of the engineers which have been done for particular products. The optimum preform shape can lead to defect free parts with minimum required tonnage and waste material [8]. Currently, the computational algorithms are developed and applied to design the optimum preform shape of very complex parts, such as the turbine blade. For example, the backward tracing algorithms together with the advanced finite element simulation were developed to determine the optimum intermediate shape in a shell nosing process to achieve the uniform wall thickness of the nosing part [9]. Furthermore, sensitivity analysis based algorithm of the optimum preform design for single stage forming process was developed. The initial shape of the billet is determined by measuring the sensitivity of design criteria, billet height, and width on the final shape of the forging to achieve complete die filling [10].

Currently, the tendency to reduce the weight of the machine elements is a big challenge. The weight reduction provides important benefits, especially for the cost reduction, but the parts must maintain good mechanical properties, lifetime service, and reliability. Therefore, achieving the lightweight components can be practically done in two ways; a) utilizing lightweight materials, such as aluminum alloys or magnesium alloys, and b) optimizing part design, such as hollow design [11].

The utilization of the hollow components often results in material and energy savings throughout the manufacturing process. Metalworking procedures are used to create hollow machine components in which the workpiece is hollowed out over its whole length (with some stock allowed for finishing). This strategy provides practical advantages in addition to the economic benefits.

In such a case of a semi-hollow stepped shaft, as shown in Figure 1, the hot backward extrusion is conventionally applied to produce such part [12]. This technique provides various advantages in terms of product quality, manufacturing rate, and cost. However, higher forming loads, lubrication costs, limiting shape complexity are the disadvantages of the backward extrusion [13]. Moreover, the backward extrusion is not commonly employed at the high temperature, because the hot backward extrusion process causes the decrease of the tool life especially at the punch corners because of the high contacting stress [14].

The forming load and the uniformity of the wall thickness are also concerned mostly in the backward extrusion. It is mainly controlled by the punch profile. The influence of the punch face slope and the punch fillet radius on the lateral and axial force was investigated in [15]. The results show that by decreasing the punch fillet radius and the punch slope, the lateral force is reduced. In contrast, the smaller punch fillet causes the increase of the axial force. Therefore, the proper punch geometry needs to be

determined. The uniformity of the wall thickness between straight and circular punch land was investigated by Danckert (2004) [16]. The different length of the punch land causes in changing the contact conditions between the punch land and the cup wall. It results in the punch off-center and variation in the cup wall thickness. Therefore, the utilization of the circular punch land reduced the maximum wall thickness variation by almost 18%. Moreover, the wall thickness uniformity is also affected by the elastic deflection of the die and container including the buckling of the punch [17]. It was recommended that the punch should be short as much as possible, and/or the forming load should be reduced below the buckling threshold of the punch during the backward extrusion to prevent buckling [18]. However, in some forging parts, the internal shape is controlled by the punch profile which depends on the geometry requirement. It is difficult to avoid or change such cases in some parts, especially for a long semi-hollow part. Therefore, the forming technique to overcome this problem needs to be developed without significantly modifying the internal punch shapes.

As seen in Figure 1, this part normally was manufactured by the hot backward extrusion. The preliminary simulation results obtained by the FEM show that the maximum forming load is about 1,500 tons, as seen in Figure 2. This such a high forming load could lead to some damages on the forming tools and the press machine. Therefore, this research aims to propose a new technique for producing the semi-hollow stepped shafts, namely, a combined bulging-piercing technique. It is composed of two main steps; bulging, and piercing- coining steps. The combined bulging-piercing technique is mainly developed to reduce the forming load in manufacturing of the long semi-hollow stepped shafts (Figure 1) and still maintain the concentricity of the parts. Three main process parameters, namely the bulging stroke (Sb), the counter-punch lifting displacement (Lc), and the friction value (m), were investigated to determine the effect on the forming load and the die filling by the FEM simulation. Only the case with the minimum forming load was selected to implement experimentally to avoid any damage which might happen in the production press and tools. Then, the die filling, wall thickness measurement, and macro etching (flowline analysis) were performed to validate the design concept and outcomes, outcomes of the load reduction, and accurate geometries.

2. Methodology

2.1. Mechanism of the combined bulging-piercing technique

The main functions of a combined bulging-piercing technique are to reduce the forming load, control the concentricity of the products, and reduce the side wall thickness variation, especially for forming the long stepped semi-hollow parts.

A schematic of this technique is shown in Figure 3. The main idea of this technique is to employ the counter-punch and the friction at the die-wall interface to control the material flow into the die cavity. Initially, the counter-punch is lift up from the counter-punch reference position by the distance, Lc. The workpiece/billet is placed on the counter-punch, and then the punch is moved down until both are in-

contact. The initial height of the billet is defined as Ti. The stroke that the punch and the workpiece are in-contact without deformation is defined as the punch reference position. Then, the punch is travelled down while the counter-punch is maintained at the reference position to upset the billet to create a bulging. The purpose of the bulging is to generate the contact pressure between the workpiece and the die. The friction at the contact will restrict the material sliding down into the die cavity during piercing. During the bulging step, the punch travels from the punch reference position and then stops at a stroke, Sb, as seen in Figure 3, whereas the counter-punch remains at the initial position. The workpiece is deformed mostly only at the radial direction and forward extrusion with a little or no backward extrusion. Consequently, the workpiece diameter gradually increases and then contacts with the die wall, as seen in Figure 4. With increasing the bulging stroke, the contact area between the workpiece and the die is increased. The forming load of this bulging step slightly increases in the first period and becomes more prominent, when the workpiece comes into contact with the die, as seen in Figure 5.

As demonstrated in Figure 3, the counter-punch immediately moves down to the counter-punch reference position after the bulging is complete. Then, the punch moves down with the traveling stroke, Sp, to pierce the workpiece as shown in Figure 4. In the piercing step, there are two forming modes; (i) the forward extrusion and (ii) the lateral extrusion, to create the hollow shape and control the concentricity of the workpiece. In Figure 4, with some evidence of the material flow velocity, the material flow during the piercing is aligned with the punch direction. While the workpiece is elongated along the wall, the bottom thickness is also reduced by material flowing outward radially. The forming load increases at the beginning and then is roughly constant until the end of the piercing stroke, as seen in Figure 5.

The coining is the last step required to control the final bottom thickness (Tc) and fulfilled the die cavity. It must be noted that even though the final bottom thickness can be attained with force increasing exponentially, the material may not be completely filled at the bottom die. However, the maximum forming load may occur in one of the two following cases; a) with the defined final bottom thickness and b) completely fulfill at the bottom die.

Thus, the total forming stroke, in Eq. 1, is composed of a) the bulging stroke, b) the piercing stroke, and c) the coining stroke, and can be controlled by two conditions; a) a constant stroke which may control the constant bottom thickness and b) a variable stroke for the material is fully filled at the bottom die.

$$S_t = S_b + S_p + S_C \quad (1)$$

$$S_{t,new} = S_{t,old} + L_c \quad (2)$$

For the constant stroke control, the counter-punch lifting displacement is fixed and the bulging stroke is only a variable parameter. The increase of the bulging stroke, not affect the maximum forming load, would mainly increase the piercing stroke but the coining stroke remains constant. However, the final product with this condition would have the bottom thickness as designed, but the material somehow not be entirely filled at the bottom die.

In contrast, the variable total forming stroke depends on the varied counter-punch lifting displacement, while the bulging stroke is constant. Therefore, the counter-punch lifting displacement variation would results mainly in changing the total forming stroke, as seen in Eq. 2. By this role, the total forming stroke increase corresponds to the increase of the piercing stroke and the decrease of the coining stroke. Hence, the maximum forming load decreases due to the less coining stroke and the more elongated workpiece. As a result, when the material is completely filled at the bottom die, the final bottom thickness would be thinner than expected.

For that reason, to achieve the forging parts with the designed thickness and fully filled shape at the bottom die, the impacts of the process parameters need to be studied

2.2. Process parameters

The FEM simulations were performed to investigate three main parameters, i.e. (i) the bulging stroke (Sb), (ii) the counter-punch lifting displacement (Cp), and (iii) the friction value (m). All the conditions are summarized in Table 1. In addition, the forming load predictions for each condition were concluded for comparison to find the applicable condition in the process.

Initially, the workpiece-die contact surface first touches at the punch stroke of 160 mm. Further, the bulging strokes were varied by 160, 180, 200, 220, and 240 mm, respectively. Then various bulging strokes proceeded continually with the piercing and the coining steps.

The initial position of the counter-punch lifting displacement is at 110 mm above the reference or zero-displacement of the counter-punch lifting, as shown in Figure 6. Then, the position change was 20 mm for every incremental step. Hence, the lifting displacement of the counter-punch was 90mm, 110 mm, and 130 mm in this numerical study. Eventually, the effect of various bulging strokes and the initial position of the counter-punch on the forming load and the bottom thickness of the workpiece were analyzed.

Here, the friction effect to the forming load was also investigated by using the friction coefficient of 0.5 and 0.7, estimated by the graphite mixture ratio of 5% and 15%, respectively, according to [19]. Specifically, the bulging stroke was 200 mm, and the counter-punch lifting displacement was 110 mm for studying this friction effect.

After the investigation, one condition that provide possibly lower forming load, would be selected to verify and implement experimentally.

Table 1
Process parameters listed for comparison of the maximum forming load

Process parameters	Investigation of process parameters		
	Bulging stroke	Counter-punch lifting displacement	Friction coefficient
Bulging stroke, mm	160, 180, 200, 220, and 240	200	200
Counter-punch lifting displacement, mm	110	90, 110, and 130	110
Friction coefficient	0.7	0.7	0.5 and 0.7

2.3. Finite element modeling

The non-isothermal FEM modeling was performed by using a half symmetric model to reduce the computational time, as seen in Figure 7. The 300,000 elements were applied to the workpiece. The forming tools are assumed as the elastic body with the tool steel properties for the hot work, AISI H13. The material property of the workpiece is a function of the temperature range (800 to 1,100°C) and the strain rate range (1.6 to 40 s^{-1}) [20], as shown in Figure 8. The chemical compositions of the workpiece are tabulated in Table 2. The heat transfer coefficient was assumed as 7 N/sec/mm/˚C and the initial temperature of the punch and die was assumed at 250 ˚C for this hot forging process simulation. The forming speed was controlled by punch velocity of 100 mm/sec.

Table 2
Chemical compositions of the AISI 1045 [21]

Elements	Carbon, C	Iron, Fe	Manganese, Mn	Phosphorous, P	Sulfur, S
Percentage	0.43 - 0.50	98.51 - 98.98	0.60 - 0.90	≤ 0.04	≤ 0.05

3. Effect Of The Process Parameters Obtained By Fem Simulation

3.1. Effect of the bulging stroke

Figure 9 shows the load-stroke curve of the counter-punch and the punch during the bulging. During the first period, the punch load slightly increases before 140 mm of the stroke. After that, the load increases with smoothly changed the slope until the stroke reaches 160 mm. Then, the roughly constant slope of the loading curve can be noticed where the forming load increases linearly due to the higher contact area between the workpiece and the die wall. It is noted that orange and green dots indicate the area of the punch-workpiece contact and the die-workpiece contact, respectively.

The forming loads in each bulging stroke (160, 180, 200, 220, and 240 mm) continued with the piercing and coining steps were explored. The results in Figure 10 shows that the increase in the bulging stroke does not significantly affect on the maximum load. It is almost constant, around 1,500 tons. Overall, the

piercing load increases almost 20 percent with increasing the bulging stroke, as seen in Figure 11 and Figure 11. Additionally, the increase in the bulging stroke dramatically causes the reduction in the piercing stroke, but the coining stroke remains constant. It is due to the limited total forming stroke. The increase of the forming load within the piercing step is because the difficulty of the material to flow in both axial and lateral directions. At 160 mm of the bulging stroke, the forward and the lateral extrusion occur concurrently from the stroke of 160 mm to 350 mm. After that, the lateral flow reduces. The material only flows in the axial direction until the forming stroke is 400 mm, as seen in Figure 13. On the other hand, the forward and lateral flow in the bulging stroke of 240 mm occurs during the stroke from 240 mm to 350 mm, as seen in Figure 14. As a result, the stroke that the material is allowed to flow in the axial and the lateral directions, is shorter than the others. Therefore, it leads to a higher piercing load.

The workpiece bottom thickness of various bulging strokes was measured during the piercing. Figure 15 demonstrates that the increase in the bulging stroke causes a reduction in the bottom thickness. The maximum deviation around 20 mm occurs at the stroke of 250 mm.

The increase of the forming load and the reduction of the final bottom thickness are plotted in Figure 16. Figure 17 illustrates the material filling into the bottom die cavity in various forming strokes. It shows that when the material is in contact with the bottom die cavity at the forming stroke of 410 mm, the forming load is increased sharply. Then, the bottom die cavity is completely filled at the stroke of 420 mm with the bottom thickness of 63 mm. At last, as designed, the final bottom thickness is achieved at the forming stroke of 422 mm.

In conclusion, when the total forming stroke is constant, the increase of the piercing stroke relies mainly on the increase of the bulging stroke but it does not lessen the maximum forming load. Therefore, the maximum forming load remains constant. The complete filling at the bottom die cavity is attained before the final bottom thickness as designed. Therefore, the punch needs to compress the workpiece further to fulfill the bottom die, resulting in a high forming load.

3.2. Effect of the counter-punch lifting displacement

The bulging load of various counter-punch lifting displacements is shown in Figure 18. The results show that the deviation of the counter-punch lifting displacement does not cause any significant change in the forming load of bulging. Contrarily, it significantly impacts the piercing and the coining loads, as seen in Figure 19. The piercing stroke significantly decreases for the counter-punch lifting displacement at 90 mm while the coining stroke increases with the extremely high forming load. The piercing stroke extends when the counter-punch lifts up to 110 mm and the coining stroke shortens. However, the maximum forming load remains unchanged. Therefore, the forming part of these two cases seems to be superior, without defects. The most extended piercing stroke is obtained in 130 mm of the counter-punch lifting displacement, and the maximum forming load is minimized from about 1,300 tons to almost 320 tons. Nonetheless, the underfilled defect occurs at the bottom of the workpiece.

In such a case of the workpiece bottom thickness, it can be seen that the higher counter-punch lifting displacement dramatically reduces the workpiece bottom thickness, as seen in Figure 20. However, the 130mm of the counter-punch lifting displacement provides the maximum reduction in the workpiece bottom thickness with the minimum forming load. The designed final bottom thickness and the die filling are not achieved yet.

In conclusion, the maximum forming load increases when the total forming stroke shortens with the total forming stroke varied. To lower the maximum forming load, the total forming stroke increases with increasing the counter-punch lifting displacement. However, a higher total forming stroke would allow some defects; the underfilled and the thinner at the final bottom thickness.

3.3. Effect of the friction coefficient

The forming load in the bulging step for various friction coefficients is illustrated in Figure 21. It reveals that the increase of friction coefficient mainly increases the maximum load of the forming punch. The maximum load increases approximately 20 percent, but the counter-punch load is relatively constant.

Figure 22 displays the forming load during the piercing and the coining steps for various friction coefficients. The results show that the overall forming load in the piercing increase about 20 percent, but, nearing the end of the stroke, the maximum load dramatically increases from 440 tons to 955 tons, or almost 50 percent.

In conclusion, it is evidence that the friction affects on the forming load, especially at the maximum forming load during the coining. Therefore, the high-performance lubricant is required to reduce the forming load and prevent the overload of the press machine capacity.

4. Experimental Results

The manufacturing process of the semi-hollow parts is illustrated in Figure 23. Firstly, the initial billet is cut by sawing machine. The square billet was selected in this study because it was available with the required billet size and avoided any initial crack at each corner due to the manufacturing process. The square cross-section of the billet is 140x140 mm and the length is 359 mm, as shown in Figure 24. Further, the rounded edges with radius of 5 mm were treated at each billet corners. Then, the billets were heated up to 1,250 ˚C by the induction heater. Before conveying to the press machine, the heated billets are passed through the high-pressure water tunnel to remove the oxide scale on their surface. For the hot forging process, the 1,250 tons hydraulic press machine is used for this production. This machine also has a cushion with 150 tons load. The water-based graphite with a ratio of 10 percent is utilized for lubrication. The forming tools are made of hot working tool steel (AISI H13) with surface hardening and nitriding surface coating.

4.1. An implementation of the combined bulging-piercing technique

The experimental conditions were selected according to the simulation results. The selection criterion was to obtain the superior forging part (complete filling and the final bottom thickness as designed) with the lower maximum load. The experiment was replicated at least ten times. Those conditions are as follows.;

The bulging stroke was fixed constant at 200 mm. The counter-punch reference position was defined to the same position as the FE modeling position and the counter-punch lifting displacement was 110 mm. The counter-punch load was limited to 70-80 tons to avoid any such as buckling and/or bending of the counter-punch. The punch and counter-punch loads were measured while the ram speed was 100 mm/sec.

However, the precise positioning and the constant forming speed in a hydraulic pressing machine are hard to control due to the precision of the control system. In this case, the counter-punch lifting was retracted to be lower than the defined position during the bulging. Even if using the PLC control, the accurate positioning control is still unsatisfactory. Therefore, to confirm that experimental results were reliable. The experiments with and without the compensated displacement of the counter-punch lifting were conducted. Moreover, the retraction of the counter-punch were monitored for every replication.

In the first experiment, the loading responses of the punch and the counter-punch (during the bulging) are shown in Figure 25 (red and green lines, respectively). The maximum forming load of the punch and the counter-punch approximately are 140 tons and 68 tons, respectively. The punch and the counter-punch loads obviously increase at the stroke of 850 mm, where the die-workpiece contact occurs. It is jumped up to almost 100 tons in case of the punch. The counter-punch load is also significantly increased from about 10 tons to almost 60 tons. Then, the forming load of the punch and the counter-punch is gradually increased until the end of the stroke. Later on, the forming load of the punch is quite constant from the ram stroke of 1,000 to 1,100 mm. After that, it is jumped up rapidly to the maximum forming load which is almost 700 tons.

It was found that the counter-punch could not hold in the position during the bulging. The counter-punch retraction during the bulging step is shown in Figure 26 and the average counter-punch retraction is shown in Figure 27. Initially, the counter-punch is lifted by 110 mm, but, at the end of the bulging stroke, the counter-punch is retracted by almost 6 mm. Therefore, it is lower from 110 mm to almost 104 mm. This causes the lower defined counter-punch lifting displacement and the higher maximum forming load. As a result, the compensation of the counter-punch lifting displacement was performed in the second experiment. The compensation of the counter-punch lifting displacement was utilized for preventing the over-retraction by 7 mm. Therefore, it was increased from 110 mm to 117 mm.

In the second experiment, the observed forming load is shown in Figure 25. The bulging load is quite similar to the first experiment which is almost 140 tons and 67 tons for the punch and the counter-punch. During the bulging step, the counter-punch is still retracted which is about 4 mm, as seen in Figure 26 and Figure 27. It was moved down from 117 mm to 113 mm. However, the last position of the counter-punch is still higher than 110 mm. Therefore, the maximum forming load during the piercing and the coining is dramatically reduced by almost 40% that was lowered from almost 700 tons to 400 tons

The flowline of the workpieces obtained from the bulging and the piercing and coining are shown in Figure 28 and Figure 29, respectively. It is evident that the workpiece's flowline is aligned with the shape of the workpiece without collapsing. As a result, the workpiece is strengthened. The desired final bottom thickness and the completely filled are also achieved.

Furthermore, the wall thickness of the workpiece was measured in different positions, as seen in Figure 30(a), and the thickness variation is shown in Figure 30(b). It can be seen that by employing this forming technique, the maximum wall thickness variation of the workpiece is about 5.5%. With this wall thickness variation, the workpiece is acceptable for proceeding to the final machining.

4.2. Comparison of the experimental results with the simulation results

The predicted forming loads obtained by the FEM simulation in various friction factors is compared with the forming load the experiment in various counter-punch lifting displacements, as shown in Figure 31. The results show that the predicted forming load during the bulging and piercing region is higher than that of the experiment, and also the predicted maximum forming load is higher than that of the experiment by almost double. The rapid increase of the forming load occurs in different region forming strokes.

The difference between the experimental and predicted forming loads might be due to the forming speed and friction factor. Maintaining a constant forming speed and displacement control for a hydraulic press machine is extremely difficult. The forming speed is directly depended on the forming load. It is slower when the forming load increases. Furthermore, to precisely control the final bottom thickness of the workpiece, the forming speed was slow down at the end of the forming stroke. As a result, the consistent forming speed was difficult to achieve in this experiment. For the friction, the precise friction factor in this process remained unclear. This method was designed with a constant friction factor which is likewise unattainable. These reasons might cause on the deviation on the predicted and the experimental forming load. However, the trend of the predicted forming load shows good agreement with the experiment. Also, this new developed technique could reduce significant forming load as well as provide a good precision of the part wall thickness and concentricity.

5. Conclusions

The combined bulging-piercing technique is proposed to manufacture the long semi-hollow stepped part at the evaluated temperature. This technique is mainly designed to reduce the forming load and the wall thickness variation and to control product concentricity. This technique was studied by the FEM simulation and then, it was implemented in the production. The conclusions of this research are as follows;

1. This technique is composed of the two main steps; a) the bulging step, and b) the piercing and coining step. The bulging aims to create the frictional contact pressure between the workpiece and the die by the use of the counter-punch. This frictional contact pressure restricts the workpiece from sliding into the die cavity. Then, the piercing is performed to create the hollow shape. The side wall thickness of the workpiece is controlled in this step. To control the final bottom thickness of the workpiece, the coning is also required. The maximum forming load is determined mainly in the coining step.
2. The maximum forming load could happen in two conditions; a) designed final bottom thickness, and b) complete filled at the bottom die cavity. These two conditions directly relate to the total forming stroke which is the combination of the bulging stroke, the piercing stroke, and the coining stroke. So, the total forming stroke can be divided into a) constant total forming stroke, and b) varied total forming stroke.
3. For the constant total forming stroke, the increase of the bulging stroke will decrease the piercing stroke and increase of the piercing load, while the counter-punch lifting displacement is fixed. However, this condition does not lower the maximum forming load. It is still remained constant. For the workpiece, this condition might lead to the workpiece with the designed final bottom thickness, and however, the underfilled defect can happen.
4. When the total forming stroke is varied and, the total forming stroke is longer by increasing the counter-punch lifting displacement. This would extend the piercing stroke and reduce the coining stroke. As a result, the maximum forming load is significantly reduced by the higher counter-punch lifting displacement. Although this condition might result in the completely filled bottom die cavity, the final bottom thickness might be undesirable.
5. The friction significantly affects on the forming load. Therefore, it must be handled with care during production.
6. According to the experimental results, it shows that the retraction of the counter-punch during the bulging leads to the increase of the maximum forming load. The changing counter-punch lifting displacement by five mm could increase the maximum forming load by almost 50%. Therefore, it is necessary to monitor the counter-punch position. If necessary, the compensation is recommended.
7. The implementation of the combined bulging-piercing technique to produce the semi-hollow stepped part was successful. The maximum forming load in the first production was almost 700 tons. Then, the counter-punch lifting displacement was compensated by seven mm in the second production, and the maximum forming load was lower by 400 tons which is about 40% reduction in the maximum forming load. Furthermore, the superior forming part was obtained. The maximum wall thickness variation was 5.5% which is desirable for the final machining.

Declarations

Funding

The authors declare that no funds, grants, or other support were received during the preparations of this manuscript.

Competing Interests

The authors have no relevant financial or non-financial interests to disclose.

Availability of data and material

The authors confirm that the data supporting the findings of this study are available within the article and/or its supplementary materials.

Code availability

Not applicable

Ethics approval

Not applicable

Consent to participate

Not applicable

Consent for publication

Not applicable

Author contributions (optional)

Not applicable

References

1. Politis, Denis J., et al., "A review of force reduction methods in precision forging axisymmetric shapes," International Journal of Advanced Manufacturing Technology, vol. 97, no. 5-8, pp. 2809-2833, 2018.
2. Kondo, Kazuyoshi, Toshimasa JITSUNARI, and Kyoichi OHGA, "Investigations on Cold Die Forging of a Gear Utilizing Divided Flow: 1st Report, Examination of applicable condition for a spur gear," Bulletin of JSME, vol. 28, no. 244, pp. 2442-2450, 1985.

3. Kondo, Kazuyoshi, and Kyoichi Ohga, "Precision cold die forging of a ring gear by divided flow method," International Journal of Machine Tools and Manufacture, vol. 35, no. 8, pp. 1105-1113, 1995.
4. T. Nakano, "Modern applications of complex forming and multi-action forming in cold forging," Journal of Materials Processing Technology, pp. 201-226, 1994.
5. Merklein, Marion, et al., "Bulk forming of sheet metal," CIRP Annals - Manufacturing Technology, pp. 725-745, 2012.
6. Merklein, Marion, et al., "Fundamental investigations on the material flow at combined sheet and bulk metal forming processes," CIRP Annals - Manufacturing Technology, pp. 286-286, 2011.
7. Nakeenopakun, N., Aue-u-lan, Y, "A proposed Common Single-Die Exchange Technique (C-SDET) to enhance production of pulleys," The International Journal of Advanced Manufacturing Technology, pp. 3625-3643, 2020.
8. Shao, Yong, et al., "Evolutionary forging preform design optimization using strain-based criterion," International Journal of Advanced Manufacturing and Technology, pp. 69-80, 2014.
9. Park, J. J., Nuno Rebelo, and Shiro Kobayashi, "A new approach to preform design in metal forming with the finite element method," International Journal of Machine Tool Design and Research, vol. 23, no. 1, pp. 71-79, 1983.
10. Zhao, Guoqun, et al., "Studies on optimization of metal forming processes using sensitivity analysis methods," Journal of Materials Processing Technology, pp. 217-228, 2004.
11. Schmieder, Felix, and Peter Kettner, "Manufacturing of hollow transmission shafts via bulk-metal forging," Journal of materials processing technology , pp. 113-118, 1997.
12. SCHULER GmbH, Metal Forming Handbook, Springer-Verlag Berlin Heidelberg, 1998.
13. ASM Handbook Volume 14A; Metalworking: Bulk Forming, Materials PArk: ASM International, 2005.
14. Saiki, Hiroyuki, et al., "Effect of the surface structure on the resistance to plastic deformation of a hot forging tool," Journal of Materials Processing Technology, vol. 113, no. 1-3, pp. 22-27, 2001.
15. Abrinia, K., and K. Gharibi, "An investigation into the backward extrusion of thin walled cans," International Journal of Material Forming, pp. 411-414, 2005.
16. J. Danckert, "The influence of the punch land in backward can extrusion," CIRP annals, pp. 227-230, 2004.
17. H. Long, "Quantitative evaluation of dimensional errors of formed components," Journal of Materials Processing Technology, pp. 591-595, 2006.
18. Labanova, Nadja, Mathias Liewald, and Alexander Felde, "Production of extremely deep sleeves by backward cold extrusion," In MATEC Web of Conferences. EDP Sciences, pp. Vol. 21, p. 02008, 2015.
19. Jeong, D. J., et al, "Effects of surface treatments and lubricants for warm forging die life," Journal of Materials Processing Technology, vol. 113, no. 1-3, pp. 544-550, 2001.
20. Manual, DEFORM V10.0.2, Columbus, Ohio, USA: Scientific Forming Technologies Corporation, 2010.
21. ASM. Handbook, Vol. 14 Forming and Forging, ASM international, 1993.

Figures

Figure 1

Geometry of the semi-hollow stepped shaft

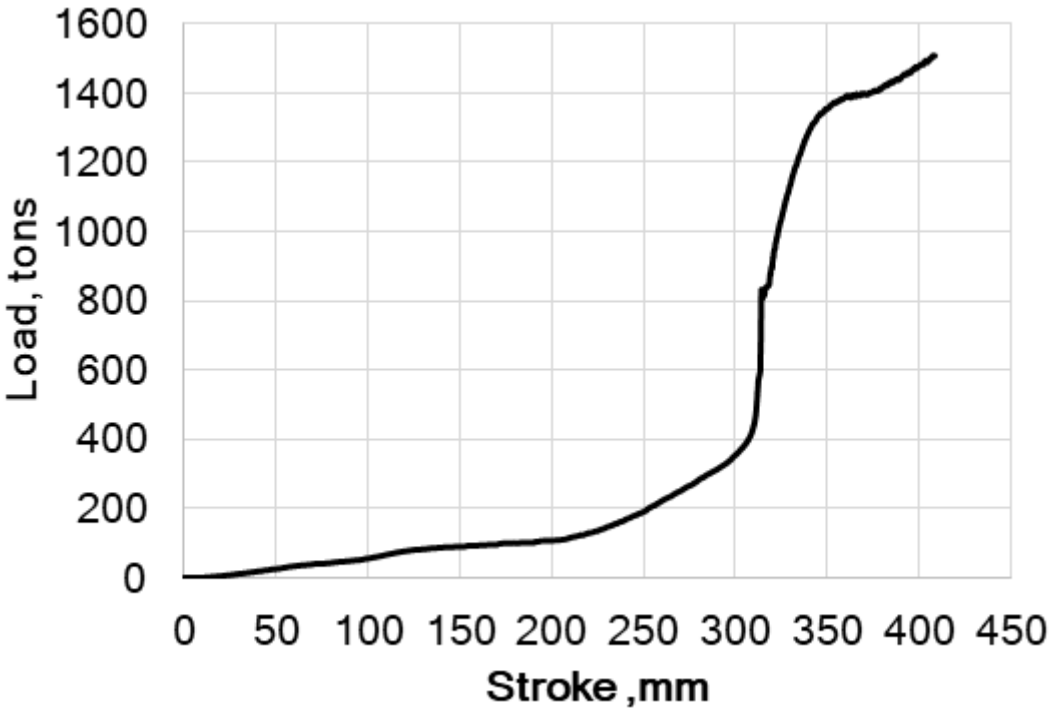

Figure 2

Predicted forming load of the conventional extrusion process

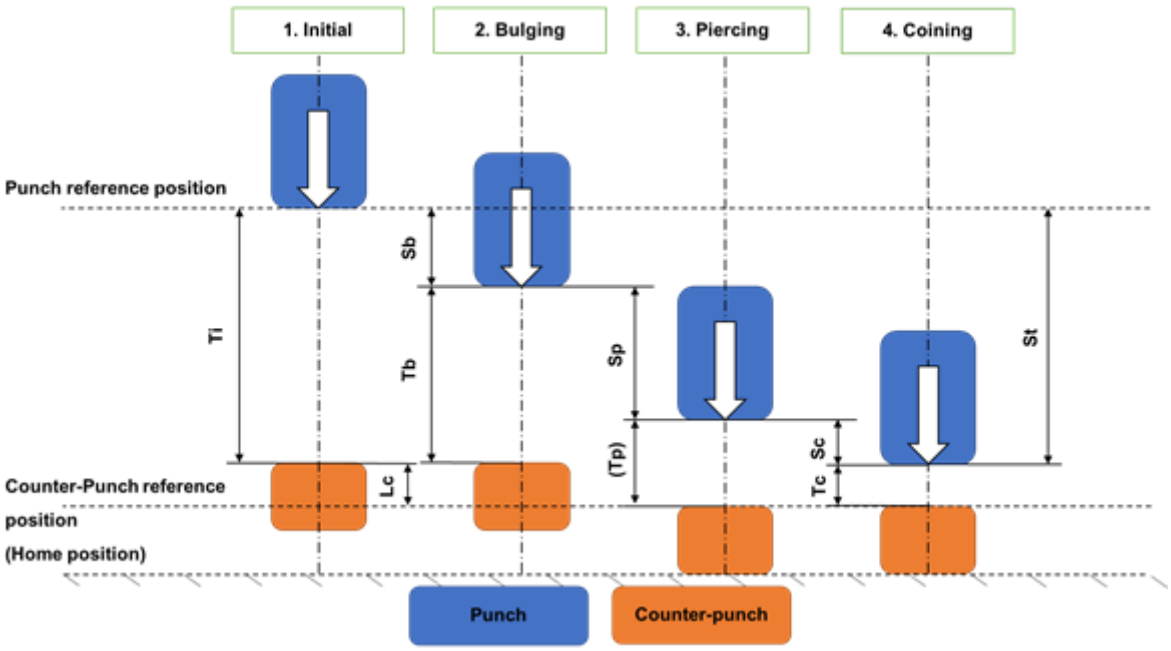

Figure 3

Schematic of the combined bulging-piercing technique

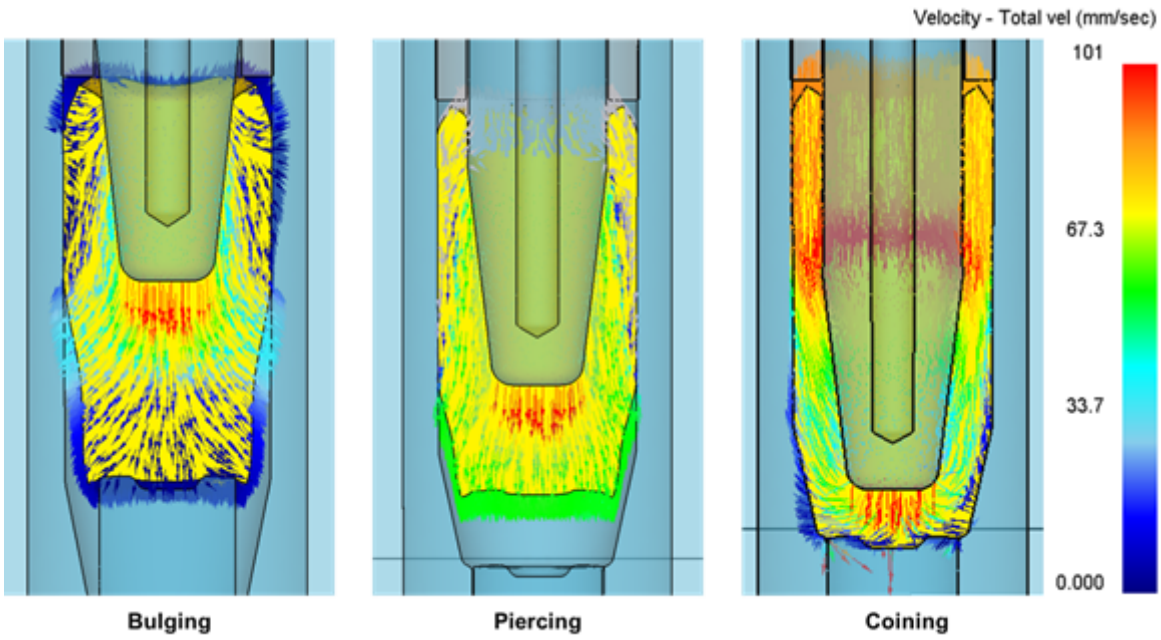

Figure 4

Velocity profile of the bulging, the piercing, and the coining

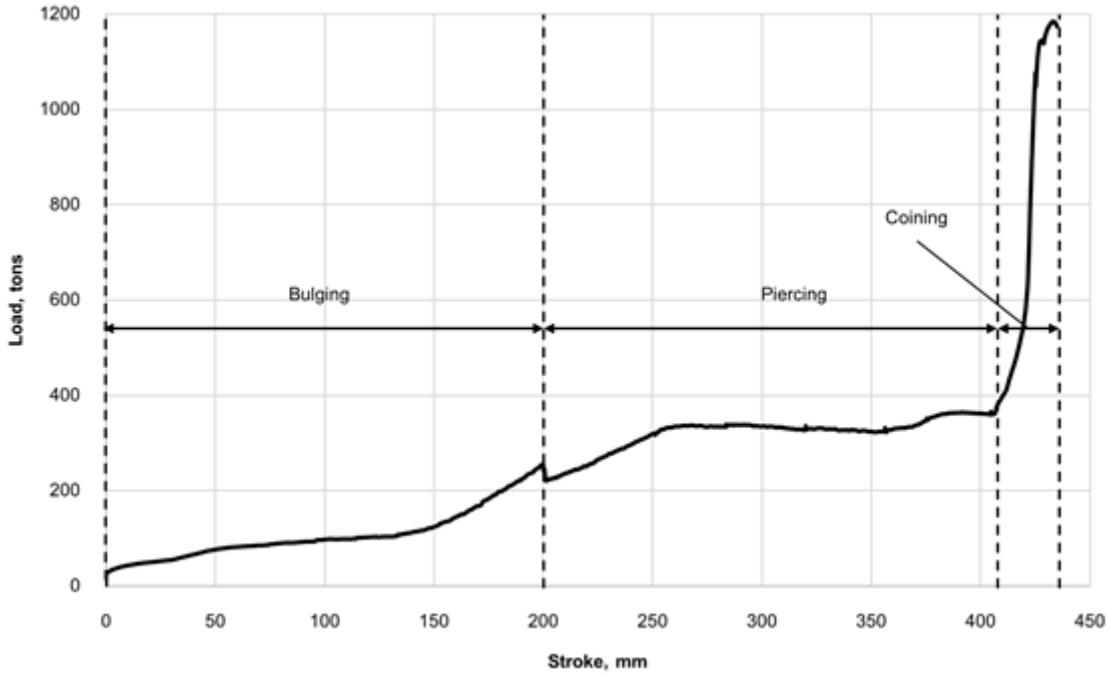

Figure 5

Load-stroke curve of the combined bulging -piercing technique

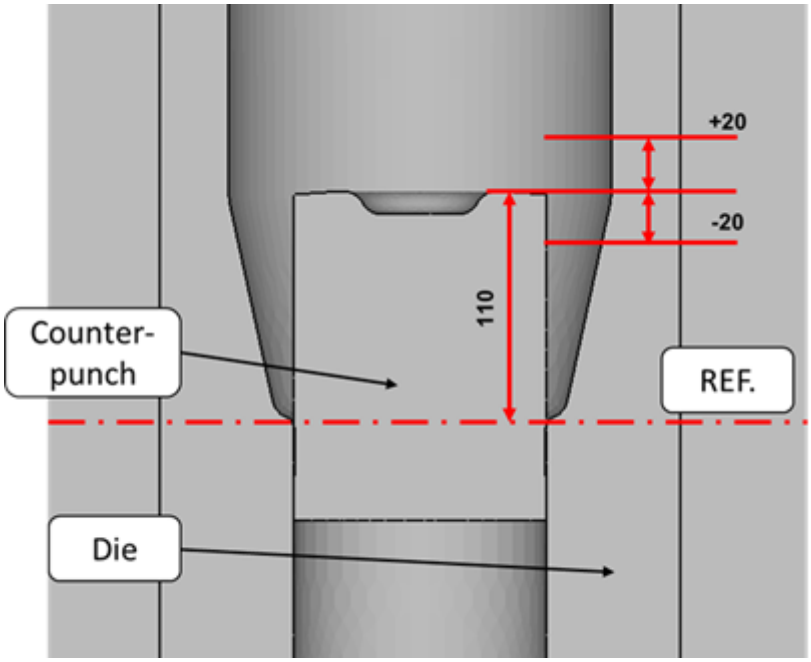

Figure 6

Schematic of the various counter-punch lifting displacements (Lc)

Figure 7

FE modeling of the hollow part

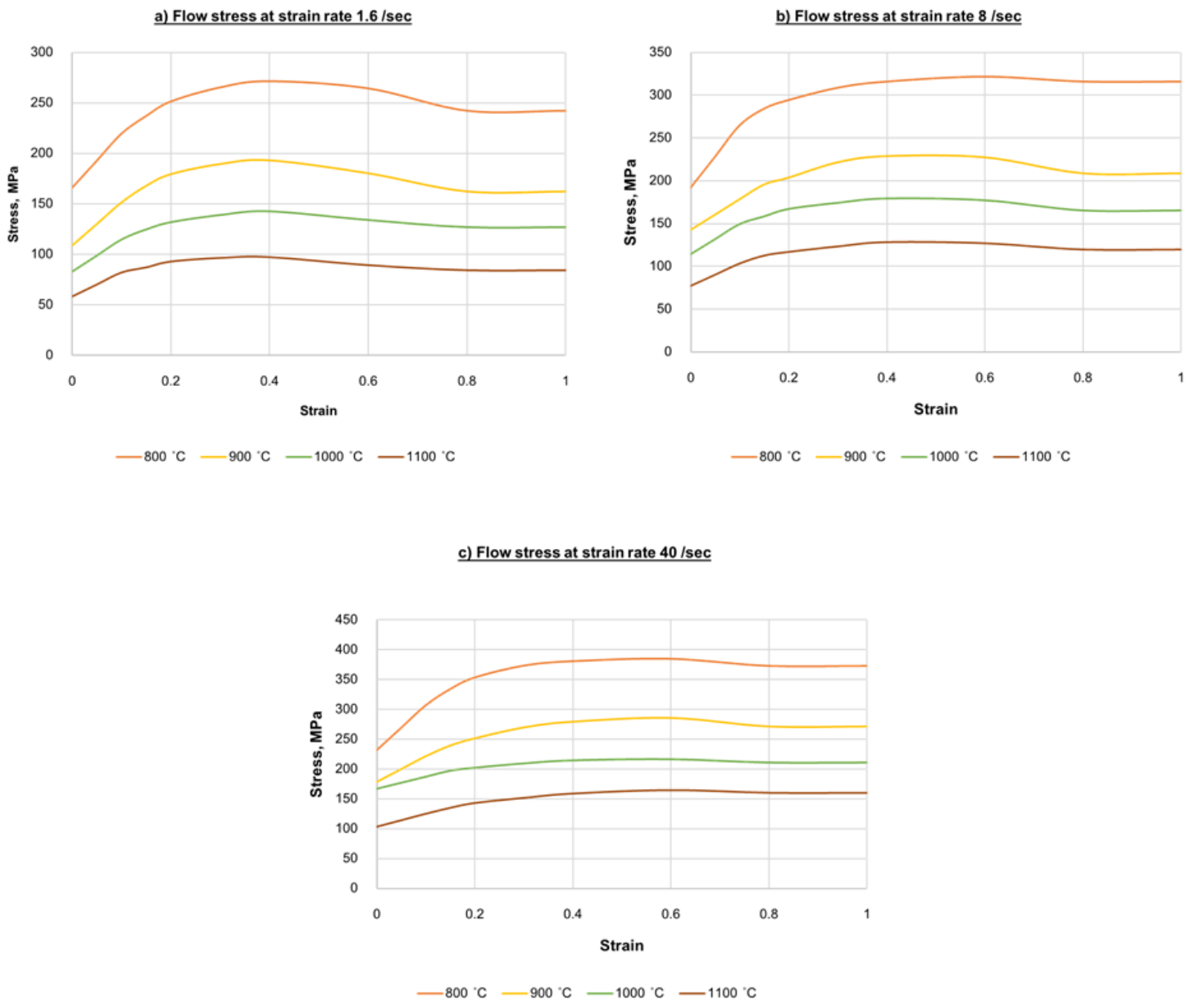

Figure 8

Flow stress of the material at various temperatures and strain rates; a) strain rate 1.6 /sec, b) strain rate 8 /sec, and c) strain rate 40 /sec [20]

Figure 9

Load-stroke curve of the punch and the counter-punch during bulging, and the contact area of the workpiece-die

Figure 10

Piercing-coining load-stroke curves of various bulging strokes

Figure 11

Load-stroke curves of the piercing of various the bulging strokes

Figure 12

Maximum load of the piercing of various the bulging strokes

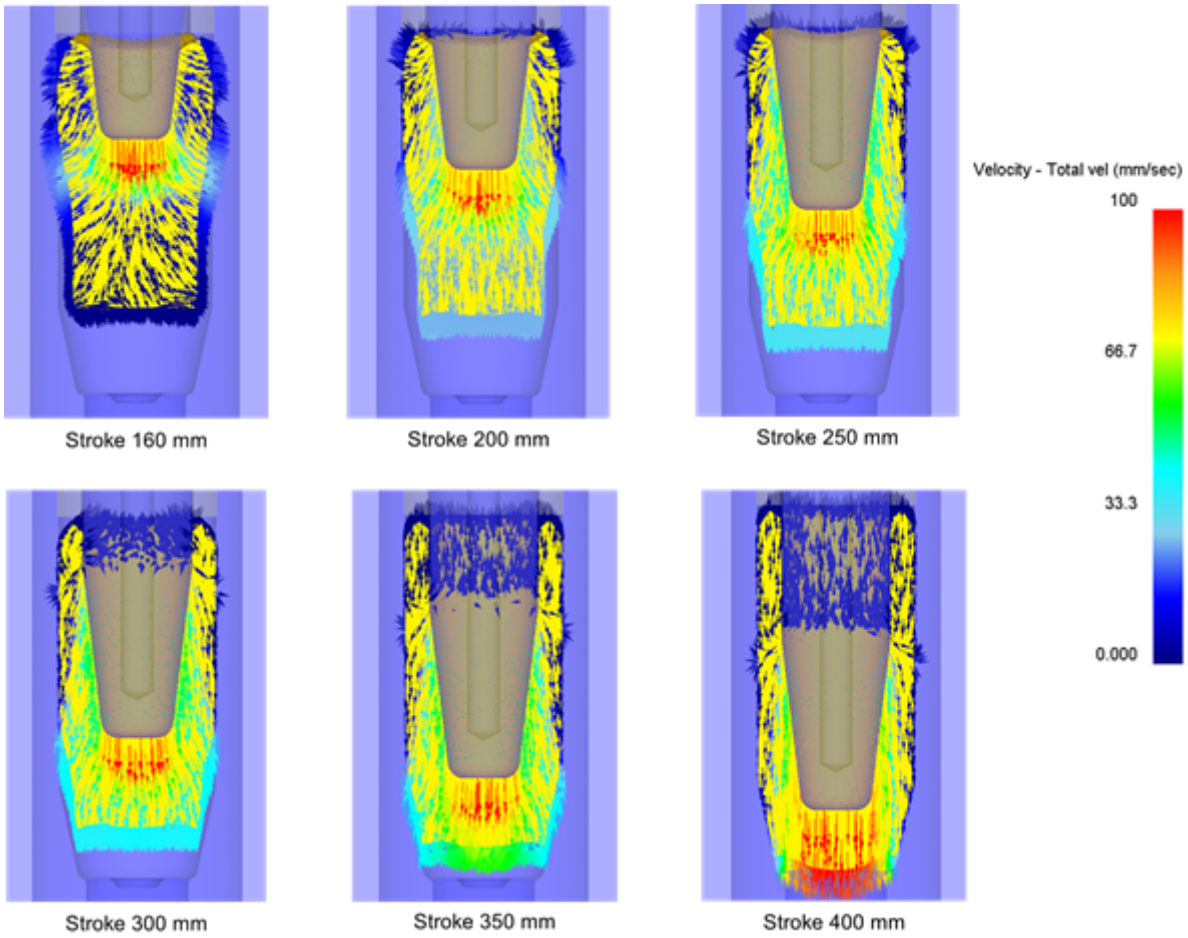

Figure 13

Material flow behavior of the workpiece during the piercing in case of the bulging stroke of 160 mm

Figure 14

Material flow behavior of the workpiece during the piercing in case of the bulging stroke of 240 mm

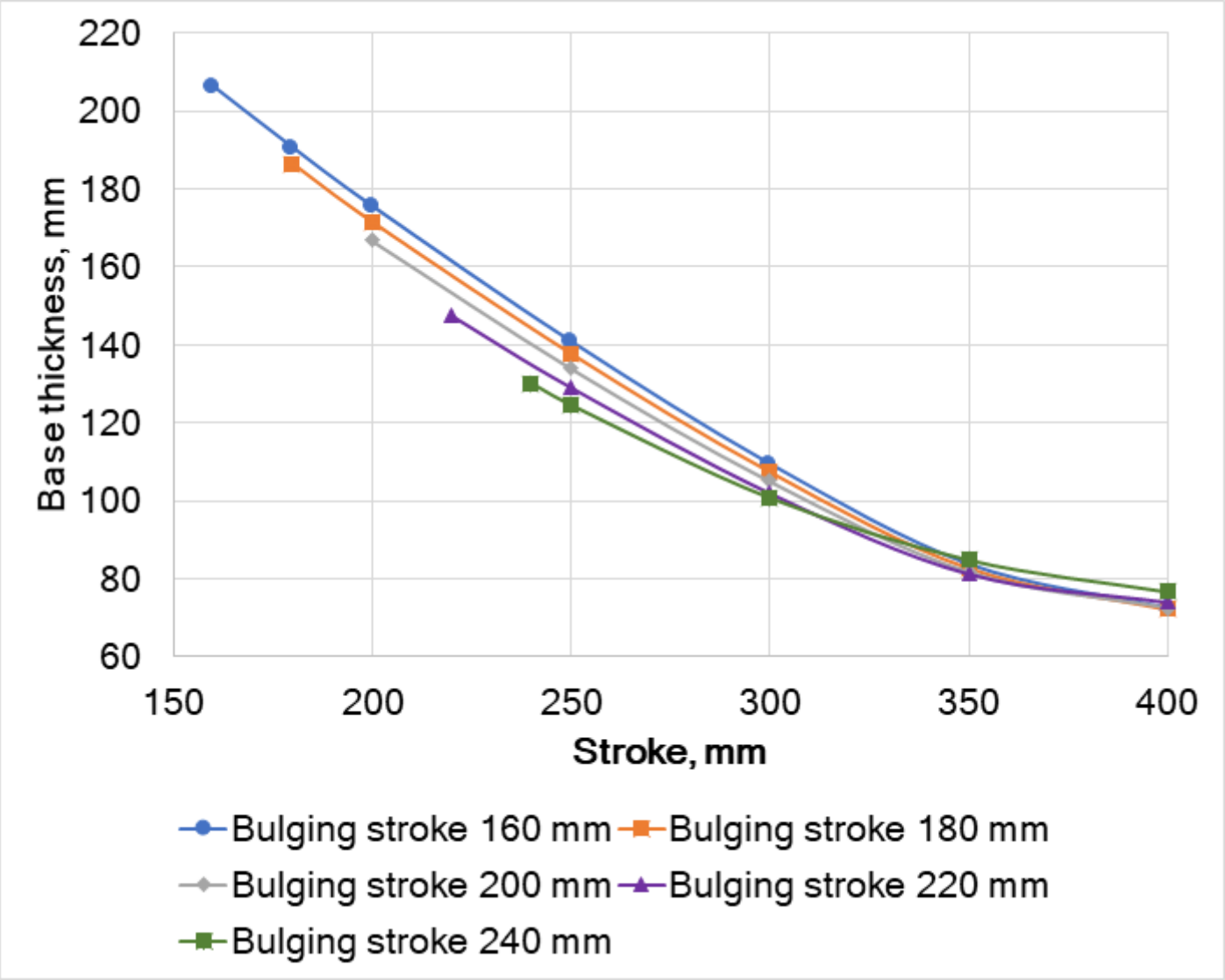

Figure 15

Bottom thickness of the workpiece in each varied bulging stroke

Figure 16

Forming load vs. final base thickness (bulging stroke of 200 mm)

Figure 17

Material filling into the bottom die cavity in various strokes

Figure 18

Bulging load of the various counter-punch lifting displacements

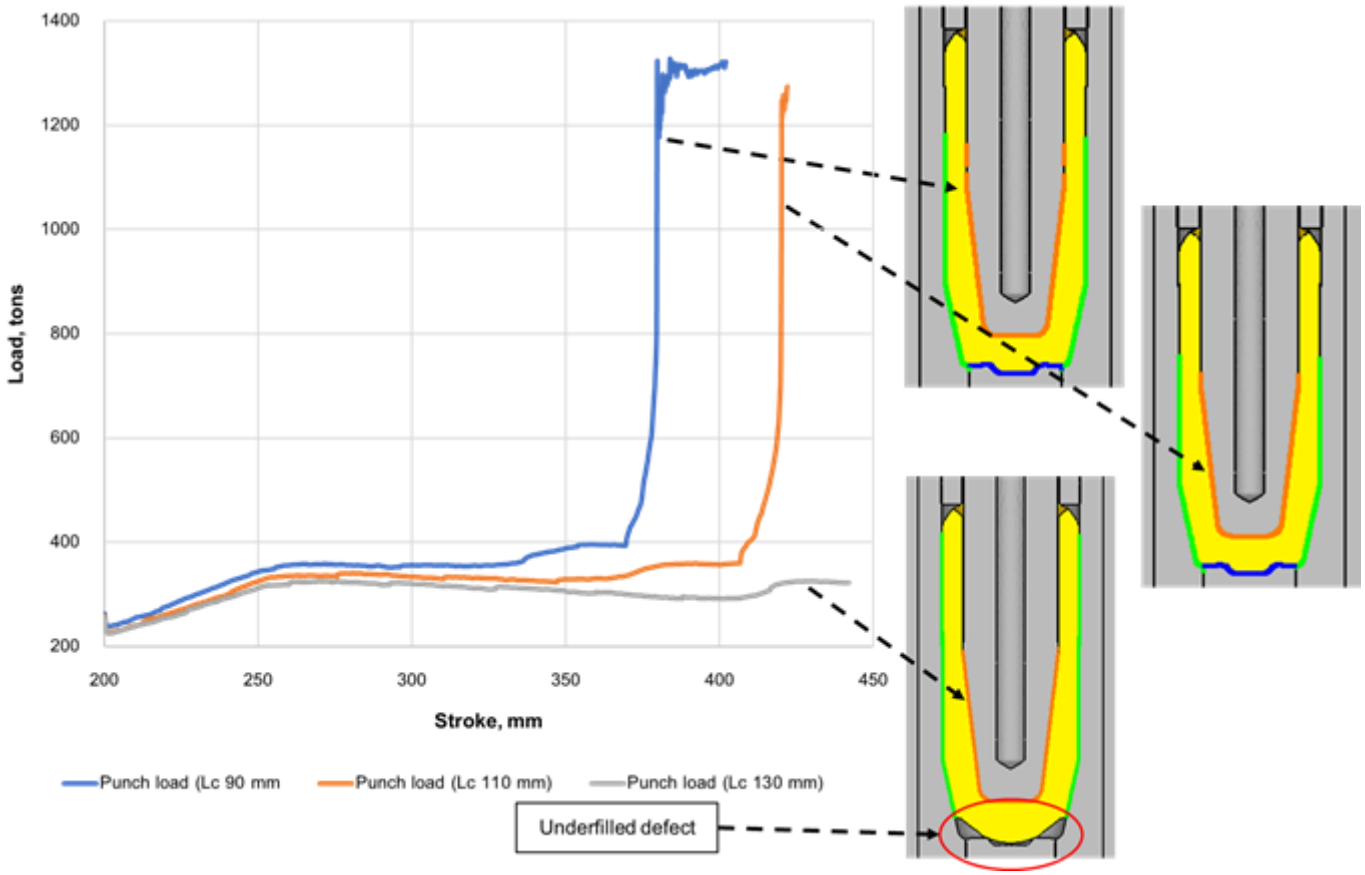

Figure 19

Piercing and coining load of various counter-punch lifting displacement

Figure 20

Reduction in the base thickness in case of various counter-punch lifting displacements

Figure 21

Bulging load-stroke curves of the punch and the counter-punch in various friction coefficients

Figure 22

Piercing load-stroke curves of the punch in case of the various friction coefficients

Figure 23

Manufacturing process of the semi-hollow part

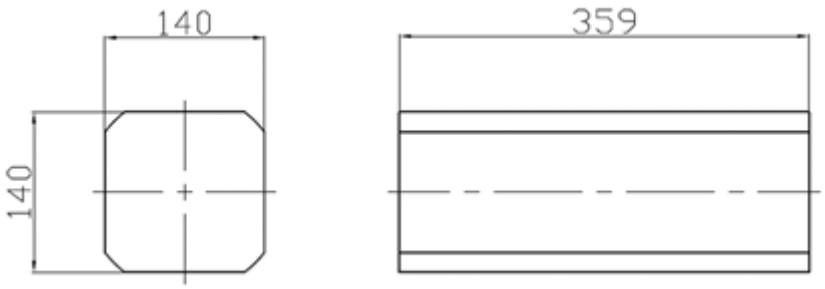

Figure 24

Initial billet dimensions

Figure 25

Forming load obtained from the experiment

Figure 26

Retraction of the counter-punch during bulging

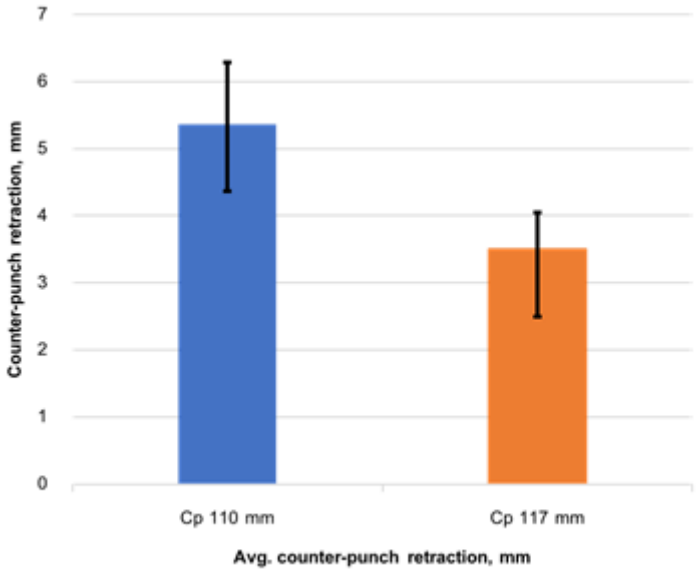

Figure 27

Averaged counter-punch retraction during bulging

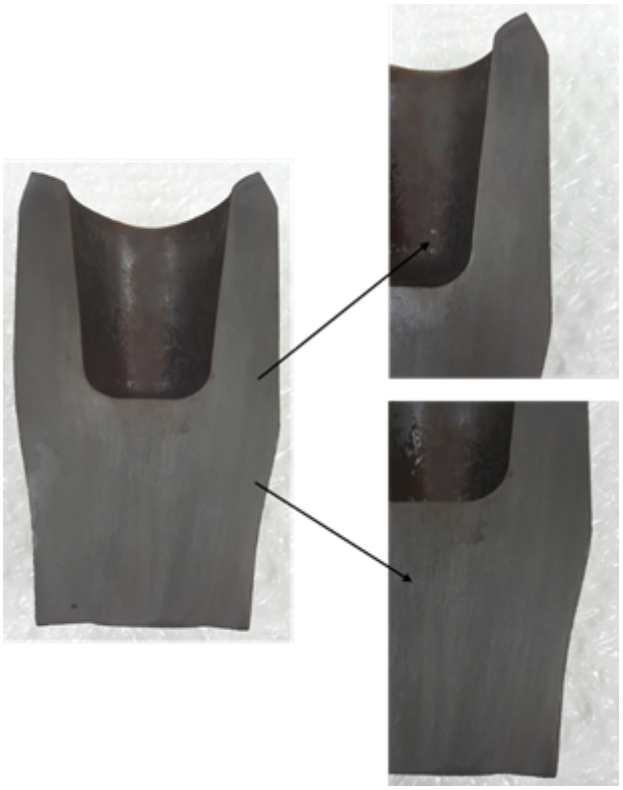

Figure 28

Bulging workpiece

Figure 29

Piercing and coining workpiece

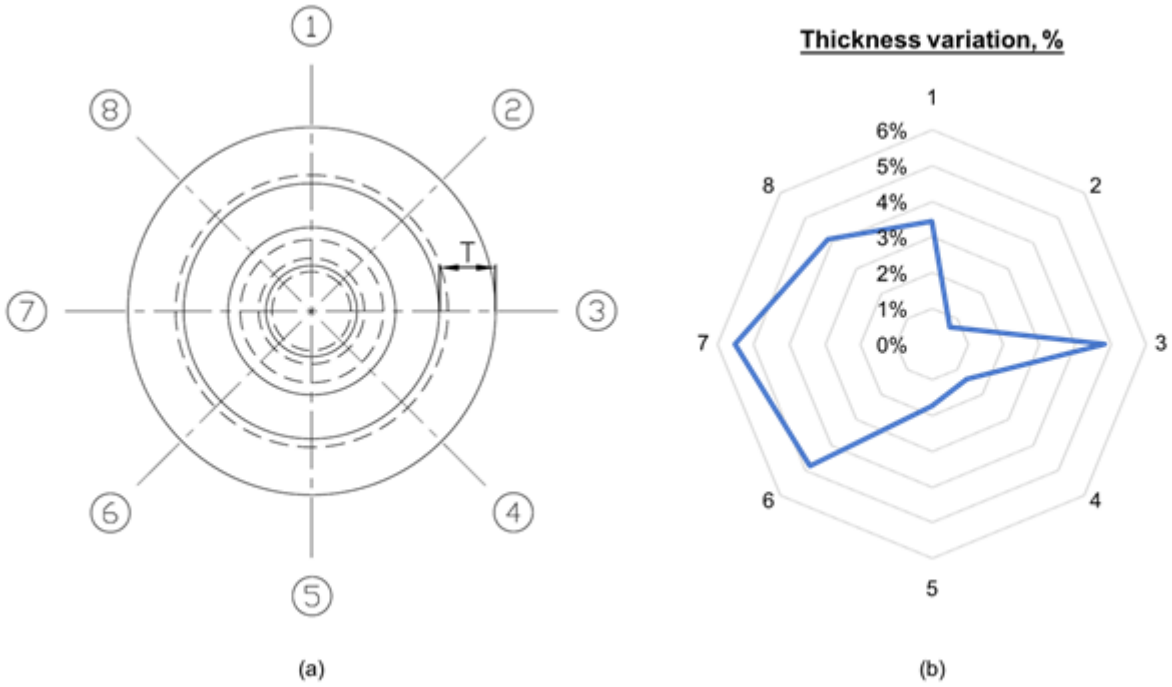

Figure 30

Measurement of the formed workpiece; (a) thickness measured positions and (b) workpiece thickness variation

Figure 31

Comparison of forming load between the experiment and the FEM simulation